

PAPER • OPEN ACCESS

## Euler-Milstein and relevant approaches for high-precision stochastic simulation of quantum trajectories

To cite this article: Nattaphong Wonglakhon *et al* 2021 *J. Phys.: Conf. Ser.* **1719** 012099

View the [article online](#) for updates and enhancements.



### 240th ECS Meeting

Oct 10-14, 2021, Orlando, Florida

**Register early and save  
up to 20% on registration costs**

Early registration deadline Sep 13

**REGISTER NOW**



# Euler-Milstein and relevant approaches for high-precision stochastic simulation of quantum trajectories

Nattaphong Wonglakhon<sup>1</sup>, Sujin Suwanna<sup>1</sup> and Areeya Chantasri<sup>1,2</sup>

<sup>1</sup> Optical and Quantum Physics Laboratory, Department of Physics, Faculty of Science, Mahidol University, Bangkok 10140, Thailand

<sup>2</sup> Centre for Quantum Computation and Communication Technology (Australian Research Council), Centre for Quantum Dynamics, Griffith University, Nathan, Queensland 4111, Australia

E-mail: nat.wonglakhon@gmail.com; sujin.suw@mahidol.ac.th;  
areeya.chn@mahidol.ac.th

**Abstract.** For quantum diffusive measurements, the system's dynamics can be described by the Itô stochastic master equation, which works well for an infinitesimal time resolution. However, in practical quantum experiments, one cannot make a time step to be infinitesimal, as it can introduce correlation of noise in time, making the Markovian assumption invalid. On the other hand, increasing a time step can cause errors from non-commuting operations describing the system's dynamics. We therefore consider implementing the Euler-Milstein and relevant approaches, namely the Itô map, the high-order completely positive map, and the quantum Bayesian, to simulate quantum trajectory for a quantum system under diffusive continuous measurements. In particular, we numerically simulate trajectories for a qubit measurement in  $z$  basis. We show the comparison of individual trajectories and their averaged trajectories among these approaches. We find that the high-order completely positive map approach yields the most accurate averaged quantum trajectory. Furthermore, we also investigate the trace distance from true stochastic quantum trajectories, comparing the four approaches using the numerical simulation. We show that, for a realistic time resolution (as in a superconducting qubit experiment), the high-order map does give the most accurate estimate of the qubit trajectories.

## 1. Introduction

The open quantum system has become an important topic in quantum information, especially when the close-system assumption is no longer applied for practical quantum experiments. We are interested in the dynamics of an open quantum system with the quantum (weak) continuous measurements, where their records are collected continuously in time, such as homodyne measurements for microwave probes used in superconducting qubit experiments [1, 2]. Evolution of the system state conditioned on the measurement results can be described by the quantum trajectory theory [3, 4]. However, in the quantum trajectory simulation, one cannot avoid the time resolution problem. If a measurement result is obtained with a really fine time resolution (too small  $\Delta t$ ), the measurement record will be correlated in time. On the other hand, if the time resolution is too coarse (too large  $\Delta t$ ), one will encounter a significant error in  $\mathcal{O}(\Delta t^2)$ .



Regarding the time resolution for continuous and diffusive quantum measurement, there have been several approaches proposed to reduce the errors of its quantum trajectory simulations. The approaches we consider in this work are: the Itô map [5], the map inspired by the Euler-Milstein method [6], the high-order completely positive map, and the quantum Bayesian approach [1, 7]. These techniques are derived from different intuitions. Therefore, in this paper, we aim to make comparison among such approaches by comparing trajectories numerically generated with fine and coarse time resolutions, and checking their agreement with the Lindblad average evolution. We consider the superconducting qubit experiment [1], where the qubit is measured in  $z$  basis, as a model for our simulation. We use the values of parameters extracted from the experiment, including the time resolution  $\Delta t = 0.016 \mu\text{s}$ , and analyse errors that can occur from different approaches mentioned above.

In quantum measurement, we consider an open quantum system  $\rho$  in the Hilbert space  $\mathcal{H}_s$  coupled to its bath (a meter)  $\rho_e = |e_0\rangle\langle e_0|$  in the Hilbert space  $\mathcal{H}_e$ . Any unitary map  $\hat{U}(t + \Delta t, t)$  for the combined system evolves the state from  $t$  to  $t + \Delta t$  in the total Hilbert space  $\mathcal{H}_s \otimes \mathcal{H}_e$ . Using the Born-Markov assumption [8], the system-bath coupling is assumed weak and the interaction time is shorter than the measurement time to avoid the influence from the bath memory and its correlation in time. In the scenario that we ignore the bath's state, we can trace the combined system state over the bath's degrees of freedom. We then obtain the unconditioned evolution describing by the Lindblad master equation [9], which is

$$\frac{\partial \rho(t)}{\partial t} = -i[\hat{H}, \rho(t)] + \mathcal{D}[\hat{c}]\rho(t), \quad (1)$$

where  $\hat{H}$  is the system's Hamiltonian, and the superoperator  $\mathcal{D}[\hat{c}]\bullet = \hat{c}\bullet\hat{c}^\dagger - \frac{1}{2}\{\bullet, \hat{c}^\dagger\hat{c}\}$  describes the *decoherence channel*. Note that we have set  $\hbar = 1$  throughout this paper.

However, for the conditioned evolution, the quantum trajectory can be found by unraveling the Lindblad master equation via *measurement operators*. The conditioned evolution can be written as

$$\rho_k(t + \Delta t) = \frac{\hat{M}_k \rho_k(t) \hat{M}_k^\dagger}{\text{Tr}[\hat{M}_k \rho_k(t) \hat{M}_k^\dagger]}, \quad (2)$$

where the measurement operator is defined as

$$\hat{M}_k = \langle e_k | \hat{U}(t + \Delta t, t) | e_0 \rangle, \quad (3)$$

using  $|e_0\rangle$  as the initial state of the bath, and  $|e_k\rangle$  is an eigenstate of the measured bath. Here,  $\text{Tr}[\bullet]$  denotes a trace operation. The measurement operator should satisfy the completeness relation, i.e.,  $\sum_k \hat{M}_k^\dagger \hat{M}_k = 1$ ; subsequently,  $\text{Tr}[\hat{M}_k \rho_k(t) \hat{M}_k^\dagger]$  yields the probability of getting the bath's state  $|e_k\rangle$  while  $\sum_k \text{Tr}[\hat{M}_k \rho_k(t) \hat{M}_k^\dagger] = 1$ . We remark that summing over all possible conditioned evolution  $\rho_k$  and taking the infinitesimal  $dt$  will recover the unconditioned evolution as in equation (1).

Let us consider an imperfect homodyne measurement (with a measurement efficiency  $\eta \in [0, 1]$ ), the evolution is conditioned on measurement records. The system's evolution can be described by the Itô stochastic master equation (SME) [3]. We here discretise the evolution with the time step  $\Delta t$ , such that the evolution is described by

$$\Delta \rho = -i[\hat{H}, \rho] \Delta t + \sum_{\mu} \mathcal{D}[\sqrt{\eta_{\mu}} \hat{L}_{\mu}] \rho \Delta t + \sum_{\nu} \mathcal{D}[\hat{V}_{\nu}] \rho \Delta t + \sum_{\mu} (\mathcal{H}[\sqrt{\eta_{\mu}} \hat{L}_{\mu}] \rho) \Delta W. \quad (4)$$

The superoperator  $\mathcal{H}$  is defined as  $\mathcal{H}[\hat{c}]\bullet = \hat{c}\bullet + \bullet\hat{c}^\dagger - \text{Tr}[\hat{c}\bullet + \bullet\hat{c}^\dagger]\bullet$ . The last term describes the stochastic *back-action*, where  $\Delta W$  is the Wiener increment [5], which has zero mean, variance  $\Delta t$ , and has a delta correlation in time. Here,  $\eta$  is the measurement efficiency, and the Lindblad operators,  $\hat{L}$  and  $\hat{V}$ , represent the measured channel and unmeasured channel, respectively.

## 2. Different approaches for quantum trajectories

For simplicity, we review the following approaches for a single measured channel  $\hat{L}$ , without the unitary evolution ( $\hat{H} = 0$ ) and assuming the measurement efficiency is perfect (no extra dephasing, i.e.,  $\eta = 1$ ). Let us begin with the conventional Itô approach derived from Itô SME equation (4). The measurement operator of this approach is defined as [3]

$$\hat{M}_I = \hat{1} - \frac{1}{2}\hat{L}^\dagger\hat{L}\Delta t + y(t)\hat{L}\Delta t, \quad (5)$$

where the measurement record is given by  $y(t)\Delta t = \langle \hat{L} + \hat{L}^\dagger \rangle \Delta t + \Delta W(t)$ . Noting that  $\langle \bullet \rangle$  represents the expectation value. This Itô map satisfies the completeness relation up to the order  $\mathcal{O}(\Delta t)$ . For the Euler-Milstein approach proposed by Rouchon and Ralph [6], the measurement operator is given by

$$\hat{M}_R = \hat{M}_I + \frac{1}{2}\hat{L}^2(y(t)^2\Delta t^2 - \Delta t), \quad (6)$$

where the second term is added to the Itô map. Since the Itô rule would make the second term vanish [5], this Euler-Milstein approach was proposed to correct the Itô stochastic differential equation by extending terms to  $\Delta W^2$ . However, this measurement operator satisfies the completeness relation up to only  $\mathcal{O}(\Delta t)$ . Therefore, we next consider the high-order completely positive map proposed by Wonglakhon, Wiseman, and Chantasri, where the measurement operator is given by

$$\hat{M}_W = \hat{M}_R + \frac{1}{8}(\hat{L}^\dagger\hat{L})^2\Delta t^2 - \frac{1}{4}y(t)[\hat{L}^\dagger\hat{L}^2 + \hat{L}\hat{L}^\dagger\hat{L}]\Delta t^2, \quad (7)$$

which includes two more terms in addition to equation (6). This measurement operator can be derived from the high order expansion in  $\Delta t$  of the unitary evolution in equation (3). Therefore, this map is more accurate for finite values of  $\Delta t$  than the aforementioned methods. It is important to note that this high-order map satisfies the completeness relation up to  $\mathcal{O}(\Delta t^2)$  and agrees with the unconditioned evolution up to  $\mathcal{O}(\Delta t^2)$  of the Lindblad evolution [10]. Finally, the last approach is the quantum Bayesian. This particular approach was introduced for Hermitian measurements. For the qubit  $z$ -measurement, the measurement operator is given by

$$\hat{M}_B \propto \exp \left[ -\frac{\Delta t}{4\tau}(\sqrt{\tau}y(t) - \hat{\sigma}_z)^2 \right], \quad (8)$$

where we have assumed  $\hat{L} = \sqrt{1/(4\tau)}\hat{\sigma}_z$  and  $\tau$  is the characteristic measurement time. The system's evolution for each approach is given by equation (2), where  $\hat{M}$  represents any of the operators  $\hat{M}_I, \hat{M}_R, \hat{M}_W$  or  $\hat{M}_B$ . We note that the full derivations for all approaches (including the unitary evolution and extra dephasing) will be published with complete details.

## 3. Numerical simulations

We implement the four approaches for qubit trajectories under the continuous  $z$ -measurement. In this paper, we consider the driven qubit with the Hamiltonian  $\hat{H} = \Omega/2\hat{\sigma}_y$ , where  $\Omega$  is the Rabi frequency. The Lindblad operators are  $\hat{L} = 1/\sqrt{4\eta\tau}\hat{\sigma}_z$  and  $\hat{V} = \sqrt{(1-\eta)/(4\eta\tau)}\hat{\sigma}_z$ , describing the measured and unmeasured channels from an imperfect measurement, respectively. We initialise the qubit state  $\rho(t_0)$  as  $z \equiv \text{Tr}[\rho\hat{\sigma}_z]$  and  $x \equiv \text{Tr}[\rho\hat{\sigma}_x]$ , where  $x$  and  $z$  are the Bloch sphere coordinates. Therefore, the Itô SME equation (4) gives

$$x(t + \Delta t) = x(t) - \Gamma x(t)\Delta t + \Omega z(t)\Delta t - x(t)z(t)(y(t) - z(t))\Delta t/\tau, \quad (9)$$

$$z(t + \Delta t) = z(t) - \Omega x(t)\Delta t + (1 - z(t)^2)(y(t) - z(t))\Delta t/\tau, \quad (10)$$

where  $\Gamma = \frac{1}{4\eta\tau}$ . Note that there is no  $y$  dynamics, since we only consider  $z$ -measurement and the qubit rotates about the  $y$ -axis in the  $x$ - $z$  plane. Here, the measurement record becomes

$$y(t)\Delta t = \frac{1}{\sqrt{\tau}}z(t)\Delta t + \Delta W(t). \quad (11)$$

Averaging the Itô SME will result in the last terms in of equations (9)-(10) vanished, giving back the usual Lindblad evolution.

As we aim to make comparison among all approaches, we therefore need to define *true* quantum trajectories as our benchmark for a fair comparison. Such trajectories can be generated using a very small time step  $dt$  (in this paper, we use  $dt = 4 \times 10^{-4} \mu s$ ), for which, all approaches give the same results. We generate true trajectories using the Itô approach as in equation (9), where the Wiener increment  $\Delta W(t)$  are generated independently with zero mean and  $\langle \Delta W^2 \rangle = dt$ . We can then construct measurement records using equation (11).

However, in real measurements, too small time step is not possible and it could violate the Markov assumption. In the superconducting transmon qubit experiment, the measurement time step was  $0.016 \mu s$  [1, 2]. Therefore, we will use  $\Delta t$ , which is  $\Delta t = 0.016 \mu s$  for our analysis. We then implement the coarse graining method to rescale the true measurement records from the time step  $dt = 4 \times 10^{-4} \mu s$  to  $\Delta t = 0.016 \mu s$ , using

$$y_{cg}(\Delta t) = \frac{dt}{\Delta t} \sum_{t'=\Delta t-dt}^{\Delta t} y(t'), \quad (12)$$

where  $y_{cg}$  is the coarse-grained record. In this paper, the comparison will be done via the trace distance, comparing the trajectories generated from the four approaches with true trajectories and the Lindblad evolution. For a qubit system, the trace distance is defined by [11],

$$D(\rho_a, \rho_b) = \frac{1}{2} |\vec{r}_a - \vec{r}_b|, \quad (13)$$

where  $\vec{r}_a$  and  $\vec{r}_b$  are vectors on the Bloch sphere for the qubit state  $\rho_a$  and  $\rho_b$ , respectively. The density matrix of a qubit is written as  $\rho = 1/2(\hat{1} + \vec{r} \cdot \vec{\sigma})$ , where  $\vec{\sigma}$  is a vector of Pauli matrices defined as  $\vec{\sigma} = (\hat{\sigma}_x, \hat{\sigma}_y, \hat{\sigma}_z)$ , and  $\vec{r} = (x, y, z)$ .

#### 4. Simulation results and discussion

The qubit trajectories are simulated from  $t_0 = 0$  to  $T_f = 1.44 \mu s$ , where the initial state is  $\rho(t_0) = \frac{1}{2}(\hat{1} + \hat{\sigma}_x)$ , i.e.,  $\vec{r}_0 = (x_0, y_0, z_0) = (1, 0, 0)$ .

##### 4.1. True trajectory and measurement record simulation

We first generate  $N = 1.5 \times 10^4$  realisations of the Wiener increments with 3,600 time steps using  $dt = 4 \times 10^{-4} \mu s$ , which are then used to simulate  $N$  true qubit trajectories. We check the average of the true trajectories and find that the trace distance comparing with the numerical Lindblad evolution is in order of  $\mathcal{O}(10^{-3})$ . The true measurement records are then constructed via equation (11).

##### 4.2. Coarse graining measurement records for quantum trajectories

In this step, we implement the coarse graining method to rescale the true measurement records from Sec. 4.1. This method will change them from 3,600 time steps to 90 time per trajectory, corresponding to changing the size of the time step from  $dt$  to  $\Delta t$ . We then implement the four approaches, using the maps  $\hat{M}_I, \hat{M}_R, \hat{M}_W$  and  $\hat{M}_B$ , to process quantum trajectories, for all  $N$  trajectories, each having 91 time steps (with the initial point  $x_0, z_0$ ).

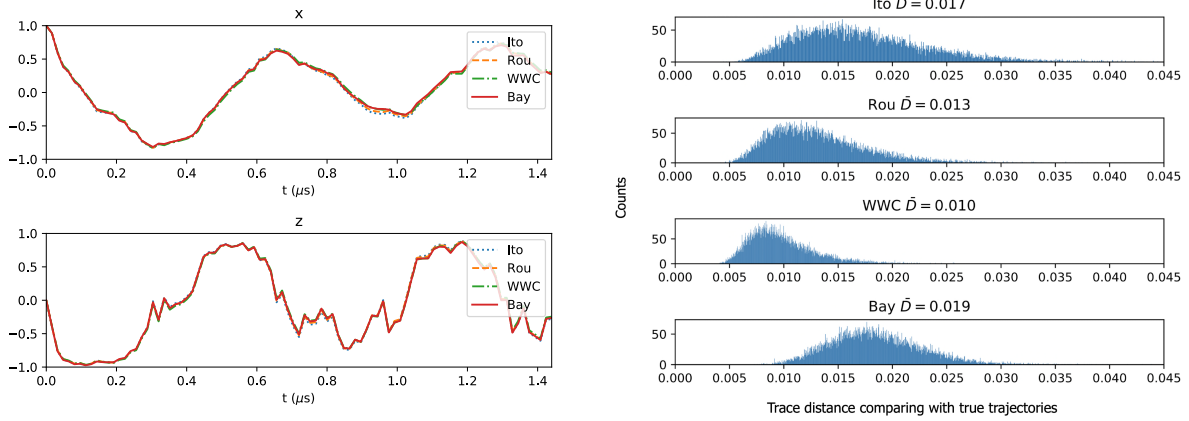


**Figure 1.** (Left) The comparison of individual trajectories calculated from the quantum Bayesian (Bay), the Euler-Milstein (Rou), the high-order completely positive map (WWC), and the Itô map (Ito) using the coarse-grained measurement records. Each record has 91 time steps with  $\Delta t = 0.016 \mu\text{s}$ . (Right) This figure displays the distribution of the trace distance comparing with the true trajectories for all approaches. The parameters are  $\Omega/2\pi = 1.08 \text{ MHz}$ ,  $\tau = 0.315271 \mu\text{s}$ , and  $\eta = 0.411932$

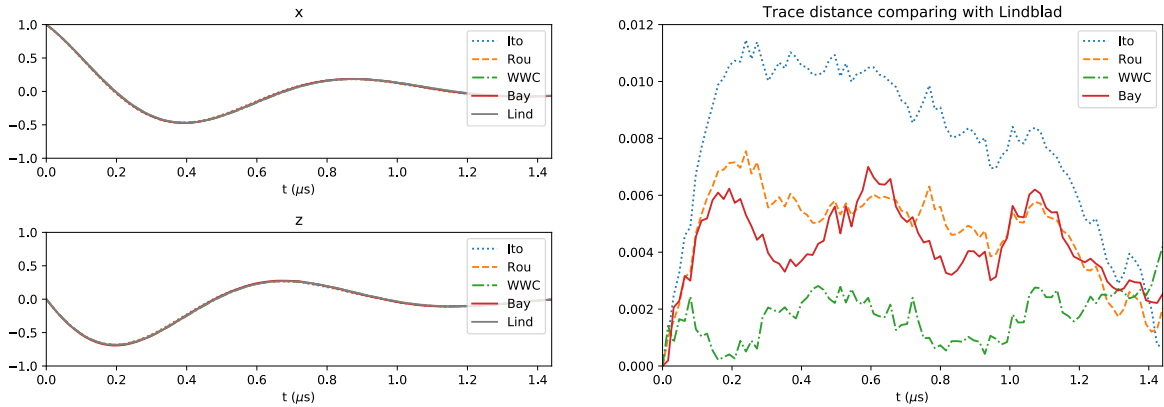


**Figure 2.** (Left) This figure displays the plot of averaged trajectory of each approach from  $N = 1.5 \times 10^4$  individual trajectories. (Right) This figure displays the changes in time of the trace distance between the averaged trajectory and the numerical Lindblad evolution.

#### 4.3. Trace distance for individual trajectories

We then analyse the generated trajectories by calculating the trace distance from the true trajectories with the relevant 90 time steps. The individual trajectories are shown in figure 1 (left). The qubit evolution is stochastic throughout its entire time of interest and all approaches yield the similar trend, though not exactly the same. We also show the distribution of the trace distance from individual trajectories over  $N$  relevant realisations for all four approaches in figure 1 (right), with the average values of the trace distance. The means of the histograms are  $\bar{D} = 0.017, 0.013, 0.010$ , and  $0.019$ , for  $\hat{M}_I, \hat{M}_R, \hat{M}_W$  and  $\hat{M}_B$ , respectively.

#### 4.4. Trace distance for averaged trajectories

Finally, we calculate the average trajectories from the  $N$  individual trajectories. As shown in figure 2 (left),  $x$  and  $z$  decay to zero as time evolves longer and all approaches give the averages close to the Lindblad solution. We calculate the trace distance of the averaged trajectory from the four approaches comparing with the numerical Lindblad evolution (calculated from solving equation (1) to second order in  $dt$ ). The calculations yield the average distances 0.008, 0.005, 0.002, and 0.004, for  $\hat{M}_I, \hat{M}_R, \hat{M}_W$  and  $\hat{M}_B$ , respectively. We also show the trace distance of averaged trajectories changes in time in figure 2 (right). It is clear the high-order completely positive map is the most accurate method, and the Itô approach is the least accurate one.

### 5. Conclusion

We have discussed the unconditioned and conditioned evolutions for continuous quantum measurements. The conditioned evolution, or the quantum trajectory, is calculated via measurement operators. We considered the evolution by four methods, which are the Itô map, the Euler-Milstein, the high-order completely positive map, and the quantum Bayesian approach. To make a fair comparison among such approaches, we simulated the true measurement records and the true trajectories for  $N = 1.5 \times 10^4$ , using the Itô approach for a really small time step  $dt$  as a benchmark for the comparison. We implemented the coarse graining method to rescale the measurement records to the larger time step  $\Delta t$ . Then, we used the coarse records to calculate the quantum trajectories using the four different maps. We investigated the trace distance comparing the generated individual and averaged trajectories with the true trajectories and the numerical Lindblad solution. The calculation results showed the high-order completely positive map  $\hat{M}_W$  is the most accurate method. Although it appears that  $\hat{M}_W$  contains more terms than the others, it still does not increase any complexity in calculations. Moreover, we can also confirm with some confidence that the time step  $\Delta t = 0.016 \mu s$  used in [1] is a good time resolution, for the simulation since the least accurate approach, the Itô approach, still gives reasonably small errors.

### Acknowledgments

NW is grateful to the Development and Promotion of Science and Technology Talents Project (DPST) for a scholarship to study at Mahidol University. AC acknowledges the support of the Griffith University Postdoctoral Fellowship scheme and Australian Research Council Centre of Excellence Program CE170100012. This research was supported by the Program Management Unit for Human Resources & Institutional Development, Research and Innovation (grant number B05F630108), Thailand.

### References

- [1] Weber S J, Chantasri A, Dressel J, Jordan A N, Murch K W and Siddiqi I 2014 *Nature* **511** 570–3
- [2] Schoelkopf R J and Girvin S M 2008 *Nature* **451** 664–9
- [3] Wiseman H M and Milburn G J 2010 *Quantum Measurement and Control* (Cambridge: Cambridge University Press)
- [4] Carmichael H J 1993 *An Open Systems Approach to Quantum Optics* (Berlin: Springer)
- [5] Gardiner C W 2004 *Handbook of Stochastic Methods for Physics, Chemistry, and the Natural Sciences* (Berlin: Springer)
- [6] Rouchon P and Ralph J F 2015 *Phys. Rev. A* **91** 012118
- [7] Korotkov A N 1999 *Phys. Rev. B* **60** 5737
- [8] Li L, Hall M J and Wiseman H M 2018 *Phys. Rep.* **759** 1–51
- [9] Lindblad G 1976 *Commun. Math. Phys.* **48** 119–30
- [10] Steinbach J, Garraway B M and Knight P L 1995 *Phys. Rev. A* **51**(4) 3302
- [11] Nielsen M A and Chuang I L 2010 *Quantum Computation and Quantum Information* (Cambridge: Cambridge University Press)